Piezoelectric-based apparatus for strain tuning

Clifford W. Hicks,[1,2] Mark E. Barber,[2] Stephen D. Edkins,[2] Daniel O. Brodsky,[2] and Andrew P. Mackenzie[1,2]
[1)] *Max Planck Institute for Chemical Physics of Solids, Nöthnitzer Straße 40, Dresden 01187, Germany*
[2)] *Scottish Universities Physics Alliance (SUPA), School of Physics and Astronomy, University of St. Andrews, St. Andrews KY16 9SS, United Kingdom*

(Dated: 18 Mar 2014)

We report the design and construction of piezoelectric-based apparatus for applying continuously tunable compressive and tensile strains to test samples. It can be used across a wide temperature range, including cryogenic temperatures. The achievable strain is large, so far up to 0.23% at cryogenic temperatures. The apparatus is compact and compatible with a wide variety of experimental probes. In addition, we present a method for mounting high-aspect-ratio samples in order to achieve high strain homogeneity.

arXiv:1403.4368v1 [cond-mat.mtrl-sci] 18 Mar 2014

INTRODUCTION

Response to uniaxial pressure can be a powerful probe of the electronic properties of materials. Uniaxial pressure directly drives anisotropic changes in the nearest-neighbor overlap integrals between atomic sites, and so will typically drive much larger changes to the electronic structure of materials than equal hydrostatic pressure. Furthermore, uniaxial pressure is directional, allowing the responses to different lattice distortions to be compared.

Many materials have been probed by uniaxial pressure. In the cuprate superconductors, for example, the transition temperature has been found to generally increase as the lattice constant ratio c/a is increased.[1] The iron pnictide superconductors $Ba(Fe,Co)_2As_2$ and $BaFe_2(As,P)_2$ are extraordinarily sensitive to small in-plane uniaxial pressures.[2] Uniaxial stress is also a useful tuning parameter for quantum dots.[3,4]

Techniques for applying controlled strains have also been developed. Adjustable strains have been applied using bending devices,[5,6] in which the sample strain is adjusted by bending a substrate, and by direct attachment to piezoelectric stacks,[7] in which the sample strain is adjusted by controlling the voltage on the stack.

The difference between applying strain and applying pressure is in the relative spring constants of the sample and apparatus. If the apparatus spring constant is much lower than that of the sample, then the controlled parameter is stress: a constant force is maintained independent of phase transitions or thermal expansion the sample might undergo. In uniaxial pressure apparatus the apparatus spring constant is usually lowered by deliberately incorporating a mechanical spring. Conversely, if the apparatus spring constant is much higher than that of the sample, the controlled parameter is strain.

In this paper we report the design and construction of a piezoelectric-based strain apparatus. Our initial motivation was to test a hypothesis on how the transition temperature of the superconductor Sr_2RuO_4 would vary on crossing between compressive and tensile strains. An ability to tension as well as compress was therefore essential. It was decided to use piezoelectric stacks, to allow rapid and precise tunability. This decision then dictated that the apparatus be built as an applied-strain rather than applied-stress device: the stroke length of the stacks, particularly at cryogenic temperatures, is miniscule, so to keep the apparatus compact it was necessary that as much of the stroke length as possible go into the sample, rather than into a force-maintaining spring.

High strain homogeneity was also an important goal. Strain inhomogeneity has been among the most significant technical difficulties in uniaxial pressure experiments. Transitions observed under uniaxial pressure have generally broadened, sometimes severely, as the pressure is increased, an indication of increasing strain inhomogeneity.[8–11] But excessive broadening risked obscuring the functional form of T_c against strain whose measurement was our aim. We embarked on the current project believing that strain homogeneity requires more careful and explicit treatment than it has normally been given, and along with the apparatus also developed a method for reliably mounting high-aspect-ratio samples within which high strain homogeneity could be obtained.

We believe that response to lattice strain is an underutilised technique. The apparatus and mounting methods we have developed are compact and reliable, and will allow new experiments across a wide range of materials.

CURRENT METHODS: UNIAXIAL PRESSURE AND DIRECT ATTACHMENT TO PIEZOELECTRIC STACKS

The most common method for achieving adjustable uniaxial strain is to clamp a sample between two anvils and apply pressure— that is, compressive stresses only. If the sample and anvil faces are in direct contact (that is, without a deformable interface layer) both faces must be polished flat. The tolerance is stringent: in typical uniaxial pressure measurements, the sample strain is $\sim$0.1%, which corresponds to $\sim$1 μm of compression over a 1-mm-long sample. To achieve high strain homogeneity, the sample and anvil surfaces need to be smooth, flat and parallel on a scale well below this $\sim$1 μm.

Even if the sample and anvil faces match perfectly, frictional locking of the sample and anvil faces can introduce strain inhomogeneity:[12] under pressure, the centre

of the sample attempts to expand according to its own Poisson's ratio, but the end faces are locked to the anvils.

Strain homogeneity can be improved by using samples with relatively high aspect ratios (length over width), and/or by incorporating deformable interface layers. A high aspect ratio allows inhomogeneous strain due to imperfections in the sample-anvil interface to decay away towards the sample center, and also allows the sample's Poisson's ratio to dominate its transverse expansion. A deformable interface layer can both smooth out the effects of bumps at the interface and reduce frictional locking. In Ref.[13], to improve strain homogeneity an aspect ratio of 2:1 was used, and gold and cadmium films were inserted at the sample-anvil interfaces.

In most uniaxial pressure systems the pressure must be set at room temperature. *In situ* adjustability has been achieved using helium-filled bellows.[10,14,15] However the bellows take up a significant amount of space, and a more compact solution would be useful.

A different technique for applying anisotropic distortion is to affix samples to piezoelectric stacks. This technique was introduced in Ref.[7] for strain tuning of semiconductors, and extended to correlated electron materials in Ref.[16]. It allows continuous adjustment of the applied strain in a very compact setup, and if the sample is sufficiently thin the applied strain can be highly homogeneous.

Two significant limitations of the sample-on-piezoelectric stack technique made it unsuitable for our experiment: limited range, and large differential thermal contraction.

In our apparatus we used common lead zirconium titanate (PZT) stacks,[17] similar to those of Refs.[7] and [16]. The datasheets indicate that at room temperature, within the manufacturer's recommended limits of -30 and $+150$ V, the total range of strain on the stacks is $\sim$0.15%. This is a small range: when we tested our own apparatus with a sample of Sr_2RuO_4, we found that the samples snapped under $\approx$0.25% tension, and could withstand at least the same amount of compression, meaning that the sample itself permitted a strain range of at least 0.5%. Microscopic VO_2 rods have been found to withstand up to $\sim$2.5% strain,[5] and, for an extreme case, it is calculated that defect-free silicon nitride could withstand tensile strains of up to $\sim$25%.[18]

The response of the piezoelectric stacks falls further as the temperature is reduced. At $\sim$1 K, we found the response per volt of our stacks (measured using a strain gauge[19,20]) to be 1/6 that at room temperature.[21] This reduced response can be partially offset by the larger voltages that can be applied at cryogenic temperatures: a 0.04% range can be achieved with voltages between -300 and $+300$ V,[7] while we achieved a 0.06% range over -180 to $+450$ V, without apparent damage to the stacks. This is still a small range, however.

Large differential thermal contraction is a challenge because PZT *lengthens* along its poling direction as it is cooled, by $\sim$0.1% between room and cryogenic temperatures.[22–24] Very few materials contract by less than 0.1% between room and cryogenic temperatures; 0.2–0.3% contraction is more typical. So, in the absence of plastic deformation of the epoxy,[25] differential thermal contraction will strain typical samples by an amount well beyond the range of the stacks, making it impossible to tune the strain through zero.

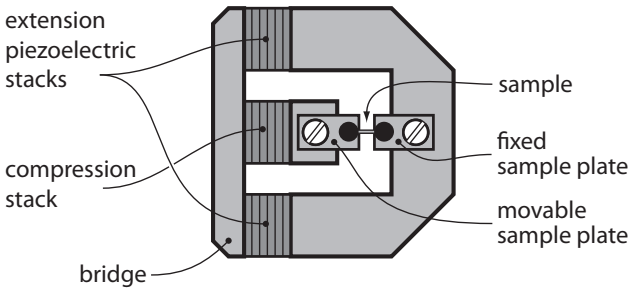

FIG. 1. An overview of our uniaxial strain apparatus.

The sample-on-stack technique is therefore best suited for measuring the linear response to small strain perturbations,[26] in circumstances where a significant nonlinear contribution is not expected.

THE UNIAXIAL STRAIN APPARATUS

A schematic overview of our uniaxial strain apparatus is shown in Fig. 1. The sample is firmly affixed with epoxy across a gap between two plates, one movable and the other fixed. The position of the movable plate is actuated by three piezoelectric stacks, which are joined by a bridge. A positive voltage applied to the central stack extends the stack and compresses the sample, while a positive voltage on the outer two stacks tensions the sample by pushing the bridge outwards. The extension and compression stacks have equal lengths, so in principle the thermal expansion of the stacks does not strain the sample.

Large sample strains are achievable. The sample strain range is $2L_{\rm stack}/L_{\rm sample}$ times the piezo strain range, where $L_{\rm stack}$ and $L_{\rm sample}$ are the stack and sample lengths, and there is a factor of two for the separate extension and compression stacks. Our first device used 4 mm-long stacks,[17] and the strained length of our samples was $\sim$1 mm. So the 0.06% stack strain range allowed a sample strain range of $\sim$0.48%, approximately centered on zero strain.

The stacks and body of the apparatus are very stiff, making it more an applied-strain than an applied-stress device. The softest part of the apparatus is the epoxy used to mount the samples. Particularly if it is relatively soft, deformation of the epoxy means that the control over the sample strain is not perfectly rigid. (Epoxy deformation is discussed further in the appendices.) But for the small samples this apparatus was designed to accept, strain remains the more tightly controlled parameter.

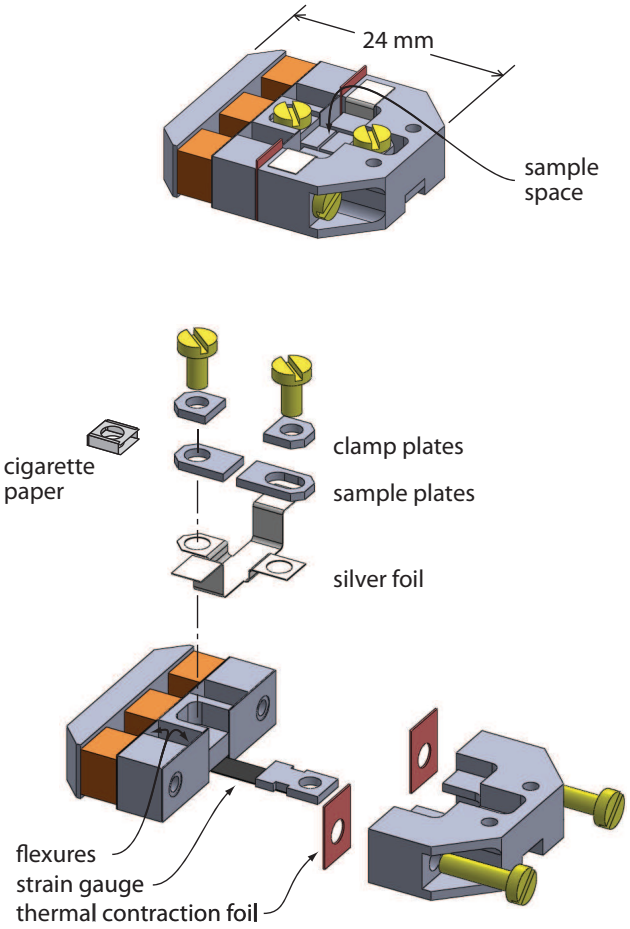

FIG. 2. Our strain apparatus.

Following Ref.[26], the applied strain is not strictly *uniaxial*, because the sample will have a nonzero Poisson's ratio. It is the stress in the sample that is more strictly uniaxial. We refer to it as a uniaxial strain apparatus because we have independent control of the strain along a single axis.

Fig. 2 shows the complete apparatus; we now describe some of the details.

Our first device was constructed out of titanium, chosen because its thermal contraction is similar to the transverse thermal contraction of the stacks.[22,23] Titanium has a low thermal contraction, however, and while the sample is not strained by differential contraction with the stacks, it is strained by differential contraction with the titanium. Therefore, copper foils (the "thermal contraction foils" in the figure) were incorporated to increase the device's thermal contraction to better match the material we studied (Sr_2RuO_4).

The flexures present a low spring constant for longitudinal motion, and a much higher spring constant for any twisting or transverse motions. They are intended to protect the stacks from inadvertent transverse forces, for example during the sample mounting process, and to reduce unwanted bending from loads not centered on the stacks.

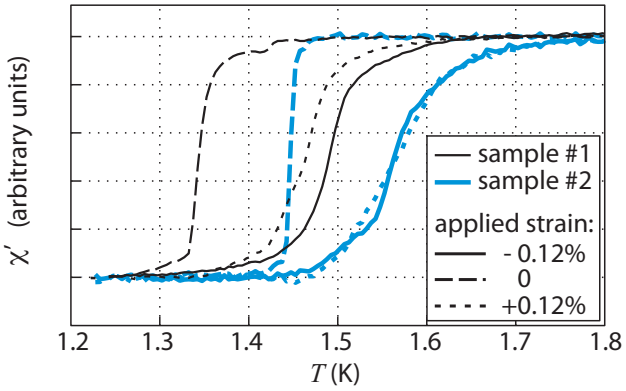

FIG. 3. Magnetic susceptibility of Sr_2RuO_4 under strains applied along a ⟨100⟩ crystal direction.

The piezoelectric stacks have significant hysteresis, particularly at large voltages, so a separate, reproducible measure of the sample strain is necessary. It is impractical to affix a strain gauge to a small sample, so the gauge is mounted across a 6-mm-wide gap beneath the sample.[19] If the gauge is suspended in this manner then it is important that it remain flat, and we found it helpful to stiffen the gauge by first epoxying it to a piece of cigarette paper. The gauge was also mounted under tension, so that it would remain flat even if the sample was strongly compressed. (In future devices with longer stacks it may be more practical to affix gauges directly to the stacks.)

Within each cool-down, the gauge so mounted provided a reproducible measure of the sample strain. It was not a perfect sensor in that its resistance had a small temperature dependence (over our measurement range of 0.5–3 K), and shifted slightly but noticably between cool-downs. Both effects required treatment during data analysis, but were not large enough to hinder measurements.

The titanium in the device is not highly conductive, with a residual resistivity ratio below ten, so a silver foil is incorporated to reduce the thermal time constant between the sample and a temperature sensor, which is mounted to a free tab of the foil. Cigarette paper can be used to electrically isolate one or both of the sample plates, if desired.

The stacks can be operated together to achieve smooth strain ramps. For example, to sweep the strain from strong compression to strong tension, the voltages on the (compression, tension) stacks might be ramped from (300, 0) to (150, 150) to (0, 300) V, thus avoiding any discontinuity in operation across zero strain.

We finish by noting that piezoelectric stacks can generate large forces. Our Sr_2RuO_4 samples were narrow, and required only ∼2 N to achieve ∼0.2% strain. The stacks we used would be able to generate at least two orders of magnitude greater force: although sample mounting will become more challenging, it would be practical to use

this design for larger samples.

Some magnetic susceptibility data for Sr_2RuO_4 under strain, using this apparatus, are shown in Fig. 3. The data show that we were able to both tension and compress the sample, and that in both cases the superconducting transition temperature increased from its unstrained value. More extensive data are given in Ref.[27].

SAMPLE MOUNTING

Common wisdom on uniaxial pressure experiments has been that epoxy is not sufficiently strong to transfer large pressures to a sample, and that high-aspect-ratio samples, in which high strain homogeneity might be obtained, would buckle under strong compression. We find that neither statement need be true.

We prepared our samples as narrow bars, typically ∼200 μm wide and ∼50 μm thick, and epoxied them across the gap between the two sample plates. Two mounted samples are shown in Fig. 4. The sample cross section should be approximately constant, for good strain homogeneity, but because the epoxy conforms to the sample there is no need for high-precision sample preparation.

Early samples were mounted as shown in panel (a), with droplets of epoxy securing the ends, and no further construction. While simple, the disadvantage of this method is its asymmetry: the sample is secured more firmly through its lower than its upper surface. A calculation presented in Appendix A shows that it is the leading ∼0.1 mm of the epoxy that transfers most of the applied load between the sample plate and sample, that is, the portions of epoxy shaded red in panel (e). Due to the asymmetry, when the sample is strained it also bends. Finite element calculations presented in Appendix B (Fig. 8) show that the strain inhomogeneity resulting from this bending can be large.

Later samples were therefore mounted as shown in Fig. 4(b): there is a rigid cap foil over the sample, so that the sample is secured with epoxy through both its lower and upper surfaces. In Fig. 3, sample #1 was mounted in this way, and sample #2 as in panel (a). The superconducting transition of sample #2 broadened considerably more under strain than that of sample #1, indicating greater strain inhomogeneity.

The epoxy we used was Stycast 2850FT. Though we did not initially appreciate this fact, the low elastic constants of this epoxy in comparison to the sample has several benefits: strain homogeneity within the exposed portion of the sample is improved, stress concentration is reduced, and the shear stress at the epoxy-sample interface is reduced. More detail on these points is presented in the appendices.

We tested the epoxy at room temperature by tensioning samples mounted as in panel (a) until fracture. We tested two samples with Epotek H20E and one with Stycast 2850FT. The samples were 70-120 μm wide and 30-100 μm thick. In all three cases, the samples snapped at tensions of ∼0.25%. Fracture occured towards the middle of the sample: it was the sample, not the epoxy, that failed. For larger samples with a lower surface-area-to-volume ratio, the stress in the epoxy will be higher and eventually the strength of the epoxy will become the limiting factor; what we have shown is that there is a practical range of parameters where the sample fails first.

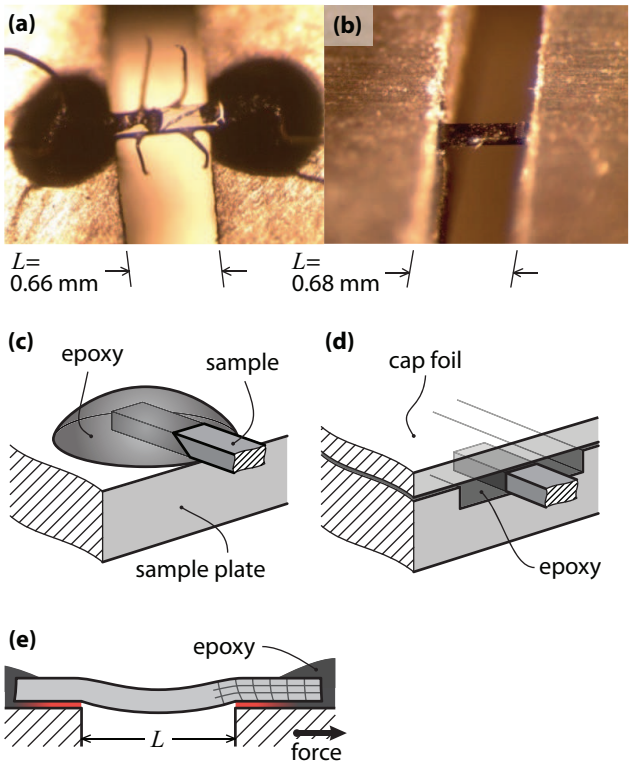

FIG. 4. (a) and (b): samples mounted across the gap between the two titanium sample plates, by two different methods, and (c) and (d): schematics of the structures in (a) and (b). The epoxy is Stycast 2850FT. In panel (a), the wires attached to the sample were used for resistance measurements prior to mounting in the strain device. (e) Illustration of how a sample mounted as in panel (a) deforms when tensioned; most of the load on the sample is transferred through the portions of epoxy shaded red.

We worked with samples with a length-to-width aspect ratio L/w as high as 7. (L throughout this article refers to the exposed length of the sample, ignoring the end portions that are embedded in epoxy.) In retrospect, this was more than necessary. As discussed in Appendix B, if the epoxy is soft and the epoxy layers sufficiently thick ($\sim$ 1/4 the sample thickness), then the strain within the exposed portion of the sample is highly homogeneous, with significant inhomogeneity (apart from any bending-induced inhomogeneity) only in the fringes immediately adjacent to the sample mounts (Appendix B, Table I). In general an aspect ratio of ∼3:1 should be sufficient.

There are also advantages in working with samples that are thin plates, with w/t (t the sample thickness)

significantly greater than one. (For Sr_2RuO_4, a layered compound, this was a natural geometry.) The surface-area-to-volume ratio is increased, reducing stress within the epoxy, and bending-induced strain inhomogeneity is reduced (Appendix B, Fig. 8). If both L/w and w/t are significantly greater than one, however, L/t can become quite large, and the risk of buckling under compression increases. We worked with samples with L/t as high as 25, which we found in retrospect to be close to buckling.

The Euler formula for the buckling load on a thin beam with both ends fixed (*i.e.*, unable to pivot) is

$$F = \frac{4\pi^2 EI}{L^2},$$

where E is the Young's modulus and I is the area moment of inertia.[28] I for a thin rectangular plate is $t^3w/12$, and the longitudinal strain is $\varepsilon = F/Ewt$. Substituting, the critical aspect ratio L/t, above which the plate buckles, is

$$\frac{L}{t} = \frac{\pi}{\sqrt{3\varepsilon}},$$

For $\varepsilon = 0.25\%$, the sample is expected to buckle for $L/t > 36$.

CONCLUSION

We have presented a design for compact, piezoelectric-based apparatus that can apply large strains to test samples, even at cryogenic temperatures. The apparatus can apply both compressive and tensile strains, a useful technological advance. We have also discussed and analysed a method for obtaining high strain homogeneity within the sample, whether using this or another distortion apparatus.

We anticipate that apparatus and methods similar to those presented here will be widely applicable. Strain-tuning is conceptually a very simple technique, and we believe that much can be learned across many systems from basic measurements such as resistivity and magnetic susceptibility as a function of sample strain. This apparatus also leaves the upper surface of the sample exposed, allowing access for spectroscopic and scattering probes. In summary, we hope that the methods that we have presented will make strain-tuning a more practical, widespread and precise technique.

ACKNOWLEDGMENTS

The authors thank Jan Bruin, Ian Fisher, Andrew Huxley and Edward Yelland for valuable discussions. They thank the UK Engineering and Physical Sciences Research Council and the Max Planck Society for financial support.

[1] F. Hardy, N.J. Hillier, C. Meingast, D. Colson, Y. Li, N. Barišić, G. Yu, X. Zhao, M. Greven and J.S. Schilling, *Phys. Rev. Lett.* **105**, 167002 (2010).
[2] H.-H. Kuo, J.G. Analytis, J.-H. Chu, R.M. Fernandes, J. Schmalian and I.R. Fisher, *Phys. Rev. B* **86**, 134507 (2012).
[3] S. Seidl, M. Kroner, A. Högele, K. Karrai, R.J. Warburton, A. Badolato and P.M. Petroff, *Appl. Phys. Lett.* **88**, 203113 (2006).
[4] M. Gong, W. Zhang, G.-C. Guo and L. He, *Phys. Rev. Lett.* **106**, 227401 (2011).
[5] J. Cao, E. Ertekin, V. Srinivasan, W. Fan, S. Huang, H. Zheng, J.W.L. Yim, D.R. Khanal, D.F. Ogletree, J.C. Grossman, and J. Wu, *Nature Nanotechnology* **4**, 732 (2009).
[6] J.H. Park, J.M. Coy, T.S. Kasirga, C.-M. Huang, Z.-Y. Fei, S. Hunter, and D.H. Cobden, *Nature* **500**, 431 (2013).
[7] M. Shayegan, K. Karrai, Y. P. Shkolnikov, K. Vakili, E. P. De Poortere and S. Manus, *Appl. Phys. Lett.* **83**, 5235 (2003).
[8] M.S. Torikachvili, S.L. Bud'ko, N. Ni, P.C. Canfield and S.T. Hannahs, *Phys. Rev. B* **80**, 014521 (2009).
[9] S.D. Johnson, R.J. Zieve and J.C. Cooley, *Phys. Rev. B* **83**, 144510 (2011).
[10] O.M. Dix, A.G. Swartz, R.J. Zieve, J. Cooley, T. R. Sayles and M. B. Maple, *Phys. Rev. Lett.* **102**, 197001 (2009).
[11] N. Takeshita, T. Sasagawa, T. Sugioka, Y. Tokura and H. Takagi, *J. Phys. Soc. Japan* **73**, 1123 (2004).
[12] X.X. Wei and K.T. Chau, *Int. J. Solids and Struct.* **46**, 1953 (2009).
[13] F. Bourdarot, N. Martin, S. Raymond, L.-P. Regnault, D. Aoki, V. Taufour and J. Flouquet, *Phys. Rev. B* **84**, 184430 (2011).
[14] U. Welp, M. Grimsditch, S. Fleshler, W. Nessler, J. Downey and G.W. Crabtree, *Phys. Rev. Lett.* **69**, 2130 (1992).
[15] C. Pfleiderer, E. Bedin and B. Salce, *Rev. Sci. Instrum.* **68**, 3120 (1997).
[16] J.-H. Chu, H.-H. Kuo, J.G. Analytis and I.R. Fisher, *Science* **337**, 710 (2012).
[17] Pch 150/5 × 5/2, Piezomechanik GmbH.
[18] S. Ogata, N. Hirosaki, C. Kocer and H. Kitagawa, *Phys. Rev. B* **64**, 172102 (2001).
[19] Vishay Micro-Measurements EK-06-250PD-10C/DP.
[20] We suppose that the gauge constant, the rate of change of gauge resistance against variation in the gauge's length, is temperature-independent. Vishay Micro-Measurements Tech Note TN-504-1 ("Strain gauge thermal output and gauge factor variation with temperature") indicates that the gauge constant for the Karma Alloy used in our gauges increases, with a linear temperature dependence, by 1.0% from 24°C to -73°C. Extrapolating to 0 K, the gauge constant would be ∼3% larger than at room temperature.
[21] This comparison is determined from the linear response at low voltages. The response rate increased gradually as the voltage increased, becoming noticeably nonlinear above ∼80 V (∼200 V) at room temperature (∼1 K).
[22] A.M. Simpson, and W. Wolfs, *Rev. Sci. Inst.* **58**, 2193 (1987).
[23] Physik Instrumente GmbH, "Piezo Material Data."
[24] The Physik Instrument piezo materials datasheet indicates a coefficient of thermal expansion for various PZT formulations of -4 to $-6 \cdot 10^{-6}$/K, along the poling direction. The thermal contraction of most materials is much diminished below ∼77 K, so multiplying this coefficient by a ∼200 K temperature range yields an expansion of 0.08 to 0.12% from room to cryogenic temperatures.
[25] Both Refs.[7] and [16] report that much less strain is transmitted from the stack to the sample at higher temperatures, 300 K for the former and above ∼100 K for the latter, than at low temperatures, suggesting significant plastic deformation of the epoxy at higher temperatures. This may hinder measurements at higher temperatures, but could have the benefit of relieving strains due to differential thermal contraction.
[26] H.-H. Kuo, M.C. Shapiro, S.C. Riggs and I.R. Fisher, *Phys. Rev. B* **88**, 085113 (2013).
[27] C.W. Hicks, D.O. Brodsky, E.A. Yelland, A.S. Gibbs, J.A.N. Bruin, K. Nishimura, S. Yonezawa, Y. Maeno and A.P. Macken-

zie, *to be published.*
[28] M. Euler, *Memoires de l'academie des sciences de Berlin* **13**, 252 (1759).
[29] The Young's modulus for loads along **x** is $E = C_{11} - C_{12}^2/(C_{11}+C_{12}) - C_{13}^2/(C_{11}+C_{13})$. It applies if the sample is free to expand and contract, following the Poisson's ratios, along **y** and **z**. If the sample is a thin plate it can probably contract along **z**, but not along **y**. In this case, the elastic constant $C_{11} - C_{13}^2/(C_{11}+C_{13})$ should be used instead of E. For realistic materials, this is not very different from E.
[30] C.E. Ojeda, E.J. Oakes, J.R. Hill, D. Aldi and G.A. Forsberg, "Temperature effects on adhesive bond strengths and modulus for commonly used spacecraft structural adhesives," Jet Propulsion Laboratory (Pasadena, CA, U.S.A.) technical report.
[31] T. Hashimoto and A. Ikushima, *Rev. Sci. Inst.* **51**, 378 (1980).
[32] J.P. Paglione, C. Lupien, W.A. MacFarlane, J.M. Perz, L. Taillefer, Z.Q. Mao and Y. Maeno, *Phys. Rev. B* **65** 220506 (2002).
[33] Emerson and Cumings Stycast® 2850FT data sheet.

Appendix A: Analytic analysis of the sample mounts.

In this appendix, we estimate analytically the load transfer length λ, the length over which the applied force is transferred between the sample plates and sample. The displacement applied by the piezoelectric stacks, and measured by the strain gauge, will be distributed over a length $L + 2\lambda$, so knowledge of λ is needed to estimate the sample strain. We also discuss the stress within the epoxy.

The parameters for our model are illustrated in Fig. 5. We make the following simplifications: (1) The sample width w is far greater than its thickness t, such that the bonding on the sides of the sample is not significant. (2) The sample plate and cap foil are perfectly rigid. (3) Shears within the sample are neglected: the strain within the sample, $\varepsilon_{xx}(x)$, is constant in both y and z. These latter two assumptions amount to supposing that the epoxy is far softer than either the sample plate or sample, which for Stycast will generally be a reasonable approximation.

Within this model, the force within the sample at position x is $F(x) = Ewt\varepsilon_{xx}$, where E is the Young's modulus of the sample.[29] F varies with x following:

$$\frac{dF}{dx} = nw\sigma(x) \approx nwC_{66,\mathrm{e}}\frac{D(x)}{d}.$$

n=1 if the sample is bonded on its lower side only, and 2 if on both the top and bottom. σ is the shear stress across the interface between the sample and epoxy, $C_{66,\mathrm{e}}$ the shear elastic constant of the epoxy, d the epoxy thickness, and $D(x)$ the displacement of the sample at position x from its unloaded position. ε_{xx} and D are related by $\varepsilon_{xx} = dD/dx$, so a differential equation for D can be readily obtained and solved. Its solution is D decaying exponentially over a length scale

$$\lambda = \sqrt{\frac{Etd}{nC_{66,\mathrm{e}}}}.$$

The elastic properties of Stycast 2850FT appear not to have been measured precisely at cryogenic temperatures. In a technical study for spacecraft applications, its Young's modulus was found to increase gradually as the temperature was reduced, but appeared to level off below ∼160 K.[30] At 150 K, it was determined to be 11½ GPa when Catalyst 24LV was used, and 16 GPa when Catalyst 9 was used. (We used Catalyst 23 LV.) The Young's modulus of Stycast 1266, an unfilled version of 2850FT, has been measured at 197 K, 77 K, and a few temperature between 77 and 2.2 K;[31] it was found to be ≈4.5 GPa for temperatures 77 K and below. If E of Stycast 2850FT behaves similarly, it may rise slightly from its 150 K value as the temperature is reduced further, before leveling off.

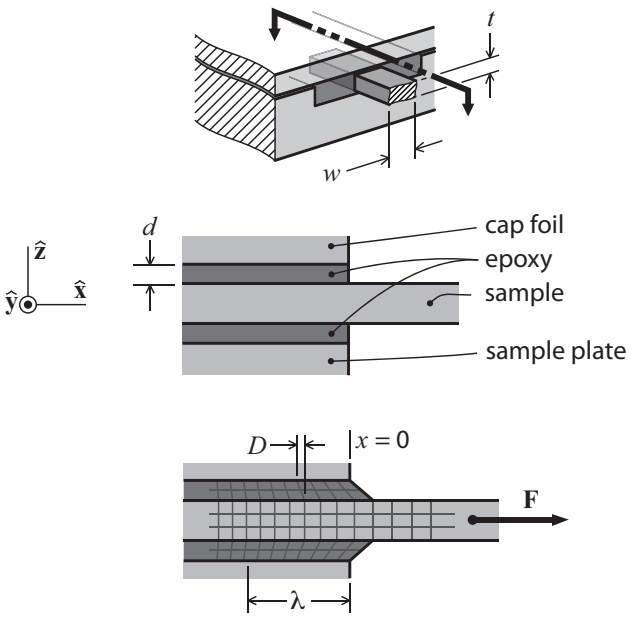

FIG. 5. A model for estimating the load transfer length λ, here for the mounting method in panel (d) of Fig. 4. When a force **F** is applied to the sample, the load is transferred to the sample plate and cap foil – both taken to be perfectly rigid – over a length scale λ. $D(x)$ is the x-dependent displacement of the sample.

The shear modulus is given by $C_{66} = E/2(1+\nu)$, where ν is Poisson's ratio. We take $E \sim 15$ GPa and $\nu \sim 0.3$, yielding $C_{66,\mathrm{e}} \sim 6$ GPa.

Sr_2RuO_4 has $E \approx 200$ GPa,[32] typical for hard oxide materials. Taking typical values $t = 50$ μm, $d = 10$ μm and $n = 2$ yields $\lambda \approx 90$ μm: it is the leading ∼0.1 mm of epoxy that transfers the applied displacement to the sample.

The shear strain within the epoxy, $\varepsilon_{xy,\mathrm{e}}$, will be maximum at the edge of the sample plate, $x = 0$. Here,

$$\varepsilon_{xy,\mathrm{e}}(0) = \frac{\varepsilon_{\mathrm{app}}\lambda}{d} = \varepsilon_{\mathrm{app}}\sqrt{\frac{Et}{ndC_{66,\mathrm{e}}}}, \qquad \text{(A1)}$$

where $\varepsilon_{\mathrm{app}}$ is the strain applied to the sample (that is, the sample strain beyond the end of the epoxy). For the above parameters, $\varepsilon_{xy,\mathrm{e}}(0)$ comes to 1.3% for $\varepsilon_{\mathrm{app}} =$ 0.2%.

The data sheet for Stycast 2850FT indicates a tensile strength of ∼50 MPa (at room temperature).[33] With $\varepsilon_{\rm app} = 0.2\%$, the shear stress in our sample mounts, using the above parameters, is $C_{66,\rm e} \times \varepsilon_{xy,\rm e} = 80$ MPa at $x = 0$. We may therefore have been close to the yield strength of the epoxy. The measurements on Stycast 1266 however indicate a fracture strain of ∼4% at low temperatures,[31] and if Stycast 2850FT performs similarly then our mounts had a comfortable margin of safety. Our measurements against strain showed almost no hysteresis, and no abrupt changes in behavior at high strains, indicating that the epoxy did not fracture or de-bond.

If failure of the epoxy becomes a significant limitation in future measurements, Eq. A1 indicates the steps to take: The sample should be bonded from both sides (so that $n = 2$). The sample should be made thin, and the epoxy layer somewhat thick. The shear stress at the interface is $\propto\sqrt{C_{66,\rm e}}$, so the best choice of epoxy appears to be one with low elastic constants, high bonding strength and high yield strain.

Appendix B: Finite-element analysis

Here we present the results of finite element simulation of a few representative cases. We discuss the load transfer length λ, strain homogeneity and sample bending.

We study four models for the sample mounts, illustrated in Fig. 6. They are: (1) "Hard epoxy:" the sample is secured on its top and bottom surfaces by a perfectly rigid epoxy. (2) "Symmetric soft epoxy:" the sample is bonded on both its top and bottom faces through thin layers of deformable epoxy to perfectly rigid surfaces (the sample plate and cap foil). (3) "Asymmetric soft epoxy:" there is a thin layer of epoxy on the lower surface only. (4) "Symmetric thick soft epoxy:" same as #2, but with thicker epoxy layers. Models #2 and 3 are close to our actual operating conditions, in which the sample was ∼200 μm wide, ∼50 μm thick and the epoxy 10–20 μm thick. Models #1 and 4 are included for comparison.

There are a few parameters to specify. For the sake of generality, we take both the soft epoxy and sample to be isotropic, with a Poisson's ratio of 0.3. Young's modulus for the soft epoxy is set to 1/10 that of the sample. The thickness of the soft epoxy layers is set to $0.25t$ for the thin layers and t for the thick layers (t the sample thickness). w is set to $4t$, and L to $6w$.

The calculations were done using a rectilinear mesh, with 15 or 16 elements spanning each of the sample thickness, sample width and epoxy thickness. The portions of the sample embedded in the epoxy were in all cases made much longer than the λ. There are no differential thermal contractions.

Fig. 7 shows some results for the strain ε_{xx}. Stress concentration in the sample is significantly reduced by using soft epoxy. In all cases, the movable sample plate

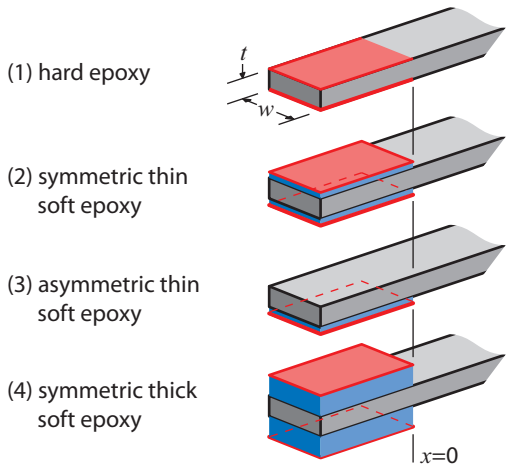

FIG. 6. Models used for finite element calculation. Red indicates the fixed faces, and blue layers of soft epoxy.

TABLE I. Lengths of the end portions of sample to exclude from measurement, to obtain a given level of strain homogeneity. Further explanation is given in the text.

% inhomogeneity	Mount model #1	#2	#4
5%	$0.4w$	$0.2w$	$0.1w$
1%	$0.8w$	$0.6w$	$0.4w$

was moved inward by 0.1% of L, but because $\lambda > 0$, the actual sample strain in the gap is less than 0.1%. In panel (c), we report λ for each calculation, determined such that to achieve an applied strain $\varepsilon_{\rm app}$ in the gap, the movable sample plate should be moved a distance $\varepsilon_{\rm app}(L + 2\lambda)$.

λ depends on parameters such as the epoxy thickness that, in practice, can be difficult to determine accurately, particularly for small samples. One disadvantage in using softer sample mounts is that greater absolute uncertainty in λ means greater uncertainty in the sample strain.

We next discuss strain homogeneity. Provided the sample does not bend (that is, the mounts are symmetric), strain inhomogeneity will decay exponentially towards the sample center. Measurements should be configured to be sensitive mainly to the sample center. The ends of the sample embedded in epoxy should clearly be excluded from measurements. A guide on how much more of the ends to exclude is given in Table I. The criterion is that at some location in the sample cross-section, the strain ε_{xx} differs from ε_{xx} at the sample centre (at $x = L/2$) by more than a given percentage. For example, using mount model #2, the outermost sample portions of length $0.2w$ should be excluded from measurement to obtain 5% strain homogeneity over the measured portion of the sample.

This is a useful result: with suitable sample mounts, the strain within almost the entire exposed section of the sample is highly homogeneous.

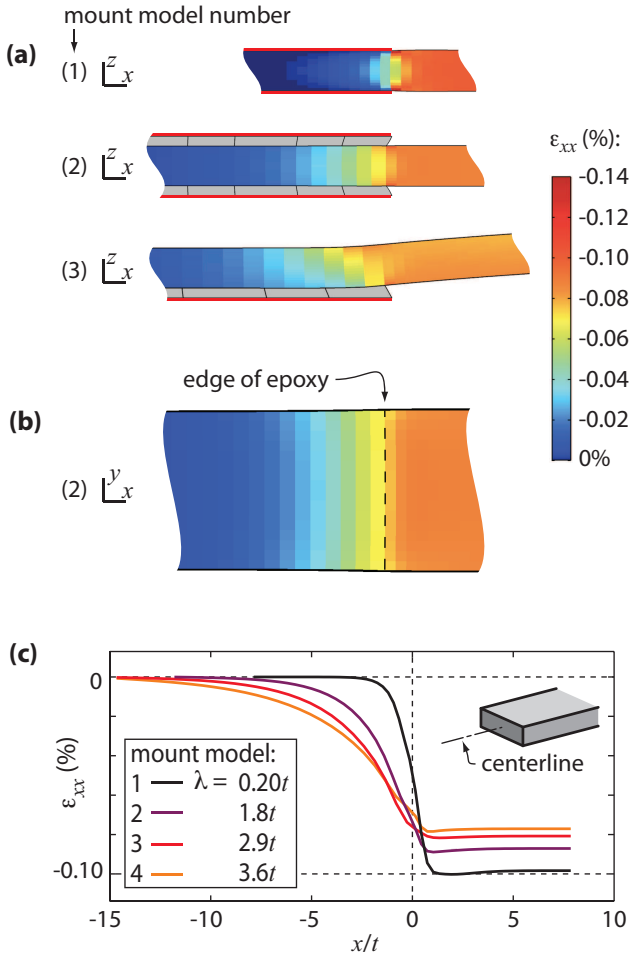

FIG. 7. Strain ε_{xx} for samples mounted as in the models of Fig. 6. In all cases, the movable sample plate was moved inward by 0.1% of L. (a) ε_{xx} in the xz center planes of samples mounted as in models (1) through (3). The red lines indicate the fixed faces. Deformations are exaggerated by a factor of 100. (b) ε_{xx} in the xy center plane for mount model (2). (c) ε_{xx} along the centerline for all the mount models. The inset shows results for λ, determined as described in the text.

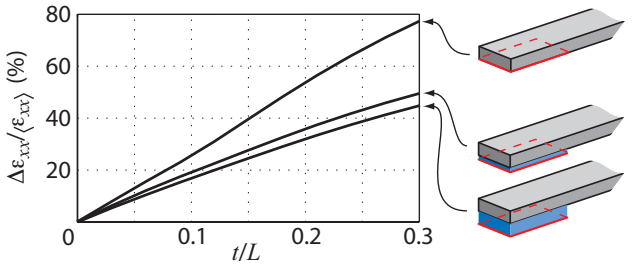

FIG. 8. Bending-induced strain inhomogeneity in the middle of the sample (at $x = L/2$) against t/L. $\Delta\varepsilon_{xx}/\langle\varepsilon_{xx}\rangle$ is the difference between ε_{xx} at the top and bottom surface, divided by the average strain through the thickness of the sample. The three cases calculated are indicated: (1) the bottom surface of the sample is held fixed; (2) and (3) the lower surface is mounted through a layer of soft epoxy, with thicknesses $0.25t$ and t.

If the sample does bend, the strain is inhomogeneous across its entire length. It is useful to know how much a typical sample might bend: it may be desirable to leave the upper surface completely exposed, and even if the mounts are intended to be symmetric between the top and bottom surfaces, imperfection in assembly will result in residual asymmetry. In Fig. 8, we show results for bending-induced inhomogeneity, as a percentage of the applied strain. Unsurprisingly, bending-induced inhomogeneity is more severe for thicker samples. The magnitude is noteworthy: $L/t = 20$, for example, is a large aspect ratio not far below the buckling limit, but even so bending could induce up to $\sim$10% inhomogeneity. Mounting with soft epoxy reduces the bending somewhat, but not dramatically. Although slightly more difficult to implement, top- and bottom-surface mounting, as illustrated in panel (d) of Fig. 4, offers clear advantages.